## 7. DIFFRACTION OVER A SINGLE ISOLATED OBSTACLE

A propagation path with a common horizon for both terminals may be considered as having a single diffracting knife edge. In some cases, reflection from terrain may be neglected as discussed in section 7.1; in other cases, ground reflections must be considered as shown in section 7.2 and appendix III. In actual situations, the common horizon may be a mountain ridge or similar obstacle, and such paths are sometimes referred to as "obstacle gain paths", [Barsis and Kirby, 1961; Dickson, Egli, Herbstreit and Wickizer, 1953; Furutsu, 1956, 1959, 1963; Kirby, Dougherty and McQuate, 1955; Rider, 1953; Ugai, Aoyagi, and Nakahara, 1963]. A ridge or mountain peak may not provide an ideal knife edge. The theory of "rounded obstacles" is discussed by Bachynski [1960], Dougherty and Maloney [1964], Neugebauer and Bachynski [1960], Rice [1954], Wait [1958, 1959], and Wait and Conda [1959]. Furutsu [1963] and Millington, Hewitt, and Immirzi [1962a] have recently developed tractable expressions for multiple knife-edge diffraction. In some cases, over relatively smooth terrain or over the sea, the common horizon may be the bulge of the earth rather than an isolated ridge. This situation is discussed in section 8.

### 7.1 Single Knife Edge, No Ground Reflections

A single diffracting knife edge where reflections from terrain may be neglected is illustrated in figure 7.1, where the wedge represents the knife edge. The diffraction loss $A(v, 0)$ is shown on figure 7.1 as a function of the parameter $v$, from Schelleng, Burrows, and Ferrell [1933] and is defined as

$$v \equiv \pm\ 2\sqrt{\Delta r/\lambda} = \pm\sqrt{(2d \tan\alpha_o \tan\beta_o)/\lambda} \qquad (7.1a)$$

or in terms of frequency in MHz:

$$v = \pm\ 2.583\ \theta\sqrt{f d_1 d_2/d} \qquad (7.1b)$$

where the distances are all in kilometers and the angles in radians. The distance

$$\Delta r \equiv r_1 + r_2 - r_o = \theta^2 d_1 d_2/(2d)$$

is discussed in section 5, and the distances $d_1$ and $d_2$ from the knife edge to the transmitter and receiver, respectively, are shown on figure 7.1. The radio wavelength, $\lambda$, is in the same units as the total path distance, $d$. The angles $\alpha_o$, $\beta_o$, and $\theta$ are defined in section 6. In this case, $h_{Lt} = h_{Lr}$, and since $d_{st} = d_{sr} = 0$, no corrections $\Delta\alpha_o$ or $\Delta\beta_o$ are required. For the line-of-sight situation, shown in figure 7.1 and discussed in section 5.1, the angles $\alpha_o$ and $\beta_o$ are both negative, and the parameter $v$ is negative. For transhorizon paths, $\alpha_o$ and $\beta_o$ are both positive and $v$ is positive.

If $v$ is greater than 3, $A(v, 0)$ may be expressed by:

$$A(v, 0) \simeq 12.953 + 20 \log v \quad \text{db} \tag{7.2}$$

The basic transmission loss, $L_{bd}$, for a knife-edge diffraction path is given by adding $A(v, 0)$ to the free space loss:

$$L_{bd} = L_{bf} + A(v, 0) \quad \text{db} \tag{7.3}$$

where $L_{bf}$ is given by (2.16). For frequencies above about 1 GHz, an estimate of the loss due to absorption (3.1), should be added to (7.3) and (7.4).

If the angles $\alpha_o$ and $\beta_o$ are small, the basic transmission loss over a knife-edge diffraction path may be written as:

$$L_{bd} = 30 \log d + 30 \log f + 10 \log \alpha_o + 10 \log \beta_o + 53.644 \quad \text{db} \tag{7.4}$$

which, however, is accurate only if $v > 3$, $d >> \lambda$, and $(d/\lambda) \tan \alpha_o \tan \beta_o > 4$.

For many paths, the diffraction loss is greater than the theoretical loss shown in (7.2), (7.3), and (7.4), because the obstacle is not a true knife edge, and because of other possible terrain effects. For a number of paths studied, the additional loss ranged from 10 to 20 db.

The problem of multiple knife-edge diffraction is not discussed here, but for the double knife-edge case, where diffraction occurs over two ridges, a simple technique may be used. The path is considered as though it were two simple knife-edge paths, (a) transmitter - first ridge - second ridge, and (b) first ridge - second ridge - receiver. The diffraction attenuation $A(v, 0)$ is computed for each of these paths, and the results added to obtain the diffraction attenuation over the whole path. When the parameter $v$ is positive and rather small for both parts of the path, this method gives excellent results. Methods for approximating theoretical values of multiple knife-edge diffraction have been developed by Wilkerson [1964].

### 7.2 Single Knife Edge with Ground Reflections

Theoretically, received fields may be increased by as much as 12 db due to enhancement, or deep nulls may occur due to cancellation of the signal by ground reflections. Reflection may occur on either or both sides of the diffracting edge. When the reflecting surface between the diffracting knife-edge and either or both antennas is more than the depth of a first Fresnel zone below the radio ray, and where geometric optics is applicable, the four ray knife-edge theory described in annex III may be used to compute diffraction attenuation. This method is used when details of terrain are known so that reflecting planes may be determined rather accurately. Using the four ray theory, the received field may include three reflected components, with associated reflection coefficients and ray path differences, in addition to the direct ray component.

When an isolated knife edge forms a common horizon for the transmitter and receiver, the diffraction loss may be estimated as:

$$A = A(v, 0) - G(\bar{h}_1) - G(\bar{h}_2) \quad \text{db} \tag{7.5}$$

where

$$\bar{h}_1 = 2.2325\, B^2(K, b^\circ)\, (f^2/a_1)^{\frac{1}{3}}\, h_{te} \cong 5.74\, (f^2/a_1)^{\frac{1}{3}}\, h_{te} \tag{7.6a}$$

$$\bar{h}_2 = 2.2325\, B^2(K, b^\circ)\, (f^2/a_2)^{\frac{1}{3}}\, h_{re} \cong 5.74\, (f^2/a_2)^{\frac{1}{3}}\, h_{re} \tag{7.6b}$$

$$a_1 = d_{Lt}^2/(2h_{te}), \quad a_2 = d_{Lr}^2/(2h_{re}).$$

The parameters $b^\circ$, K, and $B(K, b^\circ)$ are defined in subsection 8.1. The knife-edge attenuation $A(v, 0)$ is shown on figure 7.1, and the function $G(\bar{h})$ introduced by Norton, Rice and Vogler [1955] is shown on figure 7.2. Effective antenna heights $h_{te}$, $h_{re}$, and the distances $d_{Lt}$, $d_{Lr}$ are defined in section 6. In these and other formulas, f is the radio frequency in MHz.

The function $G(\bar{h}_{1,2})$ represents the effects of reflection between the obstacle and the transmitter or receiver, respectively. These terms should be used when more than half of the terrain between an antenna and its horizon cuts a first Fresnel zone ellipse which has the antenna and its horizon as focii and lies in the great circle plane. Definite criteria are not available, but in general, if terrain near the middle distance between a transmitting antenna and its horizon is closer to the ray than $0.5(\lambda d_{Lt})^{\frac{1}{2}}$ kilometers, $G(\bar{h}_1)$ should be used. The same criterion, depending on $d_{Lr}$, determines when $G(\bar{h}_2)$ should be used. When details of terrain are not known, an allowance for terrain effects, $G(\bar{h}_{1,2})$, should be used if $0.5(\lambda d_{Lt,\,Lr})^{\frac{1}{2}} > |h_{Lt,\,Lr} - h_{ts,\,rs}|/2$, where all distances and heights are in kilometers.

### 7.3 Isolated Rounded Obstacle, No Ground Reflections

Dougherty and Maloney [1964] describe the diffraction attenuation relative to free space for an isolated, perfectly conducting, rounded knife edge. The rounded obstacle is considered to be isolated from the surrounding terrain when

$$k\,h[\,2/(kr)\,]^{\frac{1}{3}} >> 1$$

where $k = 2\pi/\lambda$, $r$ is the radius of curvature of the rounded obstacle, and $h$ is the smaller of the two values $[(d_{Lt}^{\,2} + r^2)^{1/2} - r\,]$ and $[(d_{Lr}^{\,2} + r^2)^{1/2} - r\,]$.

The diffraction loss for an isolated rounded obstacle and irregular terrain shown in figure 7.3 is defined as:

$$A(v,\rho) = A(v,0) + A(0,\rho) + U(v\rho) \quad \text{db} \tag{7.7}$$

where $v$ is the usual dimensionless parameter defined by (7.1) and $\rho$ is a dimensionless index of curvature for the crest radius, $r$ in kilometers, of the rounded knife edge:

$$v\rho = 1.746\,\theta(fr)^{\frac{1}{3}} \tag{7.8}$$

$$\rho = 0.676\,r^{\frac{1}{3}} f^{-\frac{1}{6}} [\,d/(r_1 r_2)\,]^{\frac{1}{2}} \tag{7.9}$$

where, $f$ is the radio frequency in MHz, $d$ is the path distance in kilometers, and $r_1, r_2$ shown in figure 7.3 are the distances in kilometers from the transmitter and receiver, respectively to the rounded obstacle. For all practical applications, $r_1 r_2$ may be replaced by $d_1 d_2$. Where the rounded obstacle is the broad crest of a hill, the radius of curvature, $r$, for a symmetrical path is:

$$r = D_s/\theta \tag{7.10}$$

where $D_s = d - d_{Lt} - d_{Lr}$ is the distance between transmitter and receiver horizons in kilometers, and $\theta$ is the angular distance in radians (6.19). Where the ratio $\alpha_o/\beta_o \neq 1$, the radius of curvature is defined in terms of the harmonic mean of radii $a_t$ and $a_r$ defined in the next section, (8.9), and shown in figure 8.7:

$$r = \frac{2\,D_s\,d_{st}\,d_{sr}}{\theta\left(d_{st}^{\,2} + d_{sr}^{\,2}\right)} \tag{7.11}$$

In (7.7), the term $A(v,0)$ is the diffraction loss for the ideal knife edge ($r = 0$), and is read from figure 7.1. The term $A(0,\rho)$ is the magnitude of the intercept values ($v = 0$) for various values of $\rho$ and is shown on figure 7.4. The last term $U(v\rho)$ is a function of the product, $v\rho$, and is shown on figure 7.5.

Arbitrary mathematical expressions, given in annex III, have been fitted to the curves of figures 7.1, 7.3, 7.4, and 7.5 for use in programming the method for a digital computer.

The diffraction loss $A(v, \rho)$ as given by (7.7) is applicable for either horizontally or vertically polarized radio waves over irregular terrain provided that the following conditions are met:

(a) the distances $d$, $d_1$, $d_2$, and $r$ are much larger than $\lambda$,

(b) the extent of the obstacle transverse to the path is at least as great as the width of a first Fresnel zone:

$$\sqrt{\lambda d_{1,2}(1 - d_{1,2}/d)} \quad ,$$

(c) the components $\alpha_o$ and $\beta_o$ of the angle $\theta$ are less than 0.175 radians, and

(d) the radius of curvature is large enough so that $(\pi r/\lambda)^{\frac{1}{3}} >> 1$.

In applying this method to computation of diffraction loss over irregular terrain, some variance of observed from predicted values is to be expected. One important source of error is in estimating the radius of curvature of the rounded obstacle, because the crests of hills or ridges are rarely smooth. Differences between theoretical and observed values are apt to be greater at UHF than at VHF.

### 7.4 Isolated Rounded Obstacle with Ground Reflections

If a rounded obstacle has a small radius and is far from the antennas, (7.7) may neglect important effects of diffraction or reflection by terrain features between each antenna and its horizon.

Such terrain foreground effects may be allowed for, on the average, by adding a term, $10 \exp(-2.3\rho)$ to (7.7). The effect of this term ranges from 10 db for $\rho = 0$ to 1 db for $\rho = 1$. When some information is available about foreground terrain, the $G(\bar{h}_{1,2})$ terms discussed in section 7.2 may be used if more than half of the terrain between an antenna and its horizon cuts a first Fresnel zone in the great circle plane:

$$A = A(v, \rho) - G(\bar{h}_1) - G(\bar{h}_2) \quad \text{db} \tag{7.12}$$

where $A(v, \rho)$ is defined by (7.7), $\bar{h}_1$, $\bar{h}_2$ by (7.6), and the functions $G(\bar{h}_{1,2})$ are shown on figure 7.2.

When details of terrain are known, and the reflecting surfaces between the rounded obstacle and either or both antennas are more than the depth of a first Fresnel zone below the radio ray, the geometric optics four-ray theory described in annex III may be applicable. In this case, the phase lag of the diffracted field with reference to the free space field must be considered in addition to the ray path differences of the reflected components. The phase lag $\Phi(v, \rho)$ of the diffracted field is defined as

$$\Phi(v, \rho) = 90\, v^2 + \phi(v, 0) + \phi(0, \rho) + \phi(v\rho) \quad \text{degrees} \tag{7.13a}$$

where the functions $\phi(v,0)$, $\phi(0, \rho)$, and $\phi(v\rho)$ are shown on figures 7.1, 7.4, and 7.5, respectively. For an ideal knife-edge, $\rho = 0$, the phase lag of the diffracted field is

$$\Phi(v, 0) = 90\, v^2 + \phi(v, 0) \qquad \text{for } v > 0 \tag{7.13b}$$

and

$$\Phi(v, 0) = \phi(v, 0) \qquad \text{for } v \leq 0 \tag{7.13c}$$

## 7.5 An Example of Transmission Loss Prediction for a Rounded Isolated Obstacle

The path selected to provide an example of knife-edge diffraction calculations is located in eastern Colorado, extending from a location near Beulah, southwest of Pueblo, to Table Mesa north of Boulder. The common horizon is formed by Pikes Peak, with an elevation 4300 meters above mean sea level. For the purpose of these calculations Pikes Peak is considered to be a single rounded knife edge. The complete path profile is shown in figure 7.6. Table 7.1 gives all applicable path and equipment parameters and permits a comparison of calculated and actually measured values.

TABLE 7.1

Path and Equipment Parameters

| | |
|---|---|
| Carrier Frequency | 751 MHz |
| Total Great Circle Path Distance | 223.3 km |
| Great Circle Distances from Pikes Peak | |
| to Transmitter Site | 77.3 km |
| to Receiver Site | 146.0 km |
| Terminal Elevations above Mean Sea Level | |
| Transmitter Site | 1,905 m |
| Receiver Site | 1,666 m |
| Elevation of Pikes Peak | |
| Above Mean Sea Level | 4,300 m |
| Above Mean Terminal Elevation | 2,507 m |
| Transmitting Antenna Height Above Ground | 7.3 m |
| Transmitting Antenna Gain Above Isotropic (4.3 m Dish) | 26.7 db |
| Receiving Antenna Height Above Ground | 20.0 m |
| Receiving Antenna Gain Values Above Isotropic (3 m Dish) | 23.6 db |
| Polarization | Horizontal |
| Modulation | Continuous Wave |
| Transmitter Power | 445 watts |

Calculations are given for single-ray diffraction, neglecting possible specular reflections from foreground terrain.

The minimum monthly surface refractivity $N_0$ (referred to mean sea level) from figure 4.1 is 300 N-units. From Table 7.1 the terminal elevations are 1905 and 1666 m, respectively. Corresponding surface refractivity values $N_s$ are 245 and 251 N-units (4.3), and the average of these values is $N_s = 248$. In this example, $N_s$ is calculated for the terminals, as the antennas are more than 150 m below their 4300 m radio horizon. Using (4.4) or an extrapolation of figure 4.2, the effective earth radius a for $N_s = 248$ is found to be 7830 km.

The angular distance $\theta$ in radians and related parameters are calculated using (6.15) and (6.18a, b): $\theta_{et} = 0.008581$ $\theta_{er} = 0.025953$ $\alpha_{oo} = 0.021827$ $\beta_{oo} = 0.041225$. In this example $d_{st}$ and $d_{sr}$ are negligibly small, and the corrections $\Delta\alpha_o$ and $\Delta\beta_o$ (6.19a, b) can be neglected. Thus, $\alpha_{oo} = \alpha_o$, $\beta_{oo} = \beta_o$, and $\theta = 0.063052$ radians.

The free-space loss and the attenuation relative to free space are computed considering Pikes Peak to be a single isolated rounded obstacle. From a study of large-scale topographic maps, the distance $D_s$ between the radio horizons at the top of the peak is estimated to be 0.040 km. With f = 751 MHz, $d_1$ = 146.0 km, and $d_2$ = 77.3 km, we determine:

$$v = 31.73 \text{ (v is positive, as both } \alpha_o \text{ and } \beta_o \text{ are greater than zero)} \qquad (7.1b)$$

$$r = 0.6344 \text{ (7.10)}, \quad v\rho = 0.858 \text{ (7.8) and } \rho = 0.0271$$

The test described in section 7.3 shows that the assumption of an isolated obstacle is applicable. The components of basic transmission loss are then determined as follows:

$$\text{Free-space Loss } L_{bf} = 137.0 \text{ db} \qquad (2.16)$$

| | |
|---|---|
| $A(v, 0) = 43.0$ db | figure 7.1 |
| $A(0, \rho) = 6.0$ db | figure 7.4 |
| $U(v, \rho) = 5.1$ db | figure 7.5 |

Totals are: $A(v, \rho) = 54.1$ db, and from (7.3), $L_{bd} = L_{bf} + A(v, \rho) = 191.1$ db.

The average atmospheric absorption term, $A_a$, from figure 3.6 is 0.7 db. Then the total basic transmission loss value $L_{dr} = 191.8$ db, which is equal to the long-term reference value $L_{cr}$. This reference value, is strictly applicable only to those hours of the year which are characterized by a surface refractivity of approximately 250 N-units.

The expected behavior of the hourly median basic transmission loss for all hours of the year over this path can be determined using the methods described in section 10.A function $V(0.5, d_e)$ which is used with $L_{cr}$ to compute the long-term median transmission loss for a given climatic region is described in subsection 10.4. A function $Y(q, d_e)$ describes the variability relative to this long-term median that is expected for a fraction of hours q. The total cumulative distribution for this path in a Continental Temperate climate is computed as shown in subsection 10.5.

Since this is a knife-edge diffraction path, it will be necessary to calculate cumulative distributions $Y(q, d_e)$ separately for portions of the path on each side of Pikes Peak and to combine the results as described in subsection 10.8. Effective antenna heights are computed as heights above curves fitted to terrain on each side of Pike's Peak using (5.15) and (5.16). The curves are extrapolated to each antenna and to Pike's Peak. The effective heights are then the heights of the antennas and of the Peak above these curves. From Beulah to Pikes

Peak the terrain near the Peak is excluded because it is partially shadowed. Twenty-one evenly spaced points, $x_i$, from $d = 3.3$ km to $d = 70$ km were selected and the corresponding terrain heights $x_i$ were read. From (5.15b) $\overline{h} = 2100$ m, $\overline{x} = 36.6$ km, and $m = 25.5$, and the straight line fitted to terrain is

$$h(x) = 2100 + 25.5(x - 36.6) \text{ meters.}$$

At the Beulah antenna, $x = 0$ and $h(x) = 1167$ meters, at Pikes Peak $x = 75.5$ kilometers and $h(x) = 3095$ meters. The effective antenna heights are then 738 and 1205 meters (5.17). Using (10.1) to (10.3) the distances $d_L = 262.5$ km, $d_{s1} = 33.2$ km, and the effective distance $d_e$ is 34.0 km.

Similarly on the Table Mesa side much of the terrain is shadowed by the small peak at about 122 km and by the elevated area at about 202 km. The curve fit is therefore computed for the intervening terrain with $x_0 = 122.5$ km and $x_{20} = 200.5$ km. Using 21 equidistant terrain heights between these points (5.15b) gives $\overline{h} = 2025$ m, $\overline{x} = 161.5$ km, and $m = -9.3$. From (5.15a) $h(x = 75.5) = 2827$, $h(x = 223.3) = 1448$ meters. The effective antenna heights are then 1473 and 218 meters (5.17), $d_L = 222.5$, $d_{s1} = 33.2$ km, and the effective distance $d_e = 74.3$ km.

We thus have two paths in tandem where the effective distances are 34.0 and 74.3 km respectively. Cumulative distributions are obtained using figures 10.13, 10.14, 10.15, and equations (10.4) to (10.7). The frequency factors are $g(0.1, f) = 1.33$, $g(0.9, f) = 1.29$.

| | Table Mesa Side | Beulah Side | |
|---|---|---|---|
| $V(0.5, d_e)$ | 0.2 | 0 | figure 10.13 |
| $Y(0.1, d_e$, 100 MHz) | 4.7 | 1.2 | figure 10.14 |
| $Y(0.9, d_e$, 100 MHz) | -3.1 | -0.6 | figure 10.14 |
| $Y(0.1)$ | 6.3 | 1.6 | (10.6) |
| $Y(0.9)$ | -4.0 | -0.77 | (10.6) |

Using the reference value $L_{cr} = 191.8$ db and the ratios given in (10.7) the predicted cumulative distributions for both portions and for the entire path are tabulated below:

$L_b(q)$ in db

| q | Table Mesa | Beulah | Entire Path |
|---|---|---|---|
| 0.0001 | 170.6 | 186.5 | 170.1 |
| 0.001 | 174.4 | 187.4 | 173.8 |
| 0.01 | 179.0 | 188.6 | 178.6 |
| 0.1 | 185.3 | 190.2 | 184.8 |
| 0.5 | 191.6 | 191.8 | 191.3 |
| 0.9 | 195.6 | 192.6 | 195.5 |
| 0.99 | 198.9 | 193.2 | 199.0 |
| 0.999 | 201.2 | 193.7 | 201.3 |
| 0.9999 | 203.2 | 194.0 | 203.2 |

The cumulative distribution of predicted basic transmission loss for the entire path was obtained by convoluting the distributions for each part of the path, as described in subsection 10.8. This cumulative distribution is shown graphically in figure 7.7 together with a distribution derived from measurements over this path, reflecting 1056 hours of data obtained in 1960 and 1962.

The confidence limits on figure 7.7 were derived assuming that

$$\sigma_c^2(q) = 16.73 + 0.12\ Y^2(q)$$

where the variance $\sigma_c^2(0.5) = 12.73\ db^2$ given in (V.40) has been increased by $4\ db^2$ to allow for equipment and reading errors.

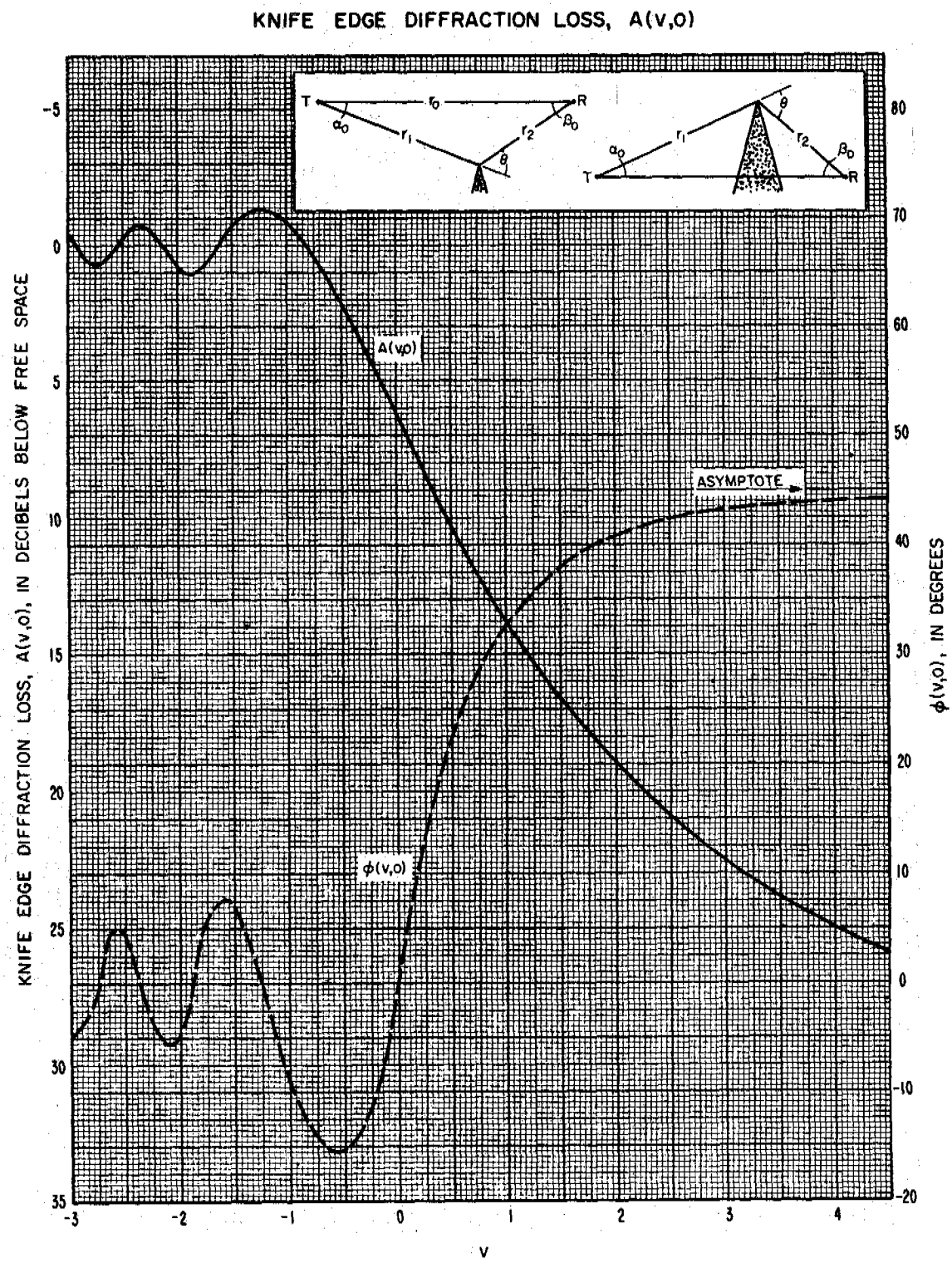
KNIFE EDGE DIFFRACTION LOSS, A(v,0)
KNIFE EDGE DIFFRACTION LOSS, A(v,0), IN DECIBELS BELOW FREE SPACE
φ(v,0), IN DEGREES
v
A(v,0)
φ(v,0)
ASYMPTOTE
T
R
r0
r1
r2
α0
β0
θ
-5
0
5
10
15
20
25
30
35
80
70
60
50
40
30
20
10
0
-10
-20
-3
-2
-1
0
1
2
3
4

Figure 7.1

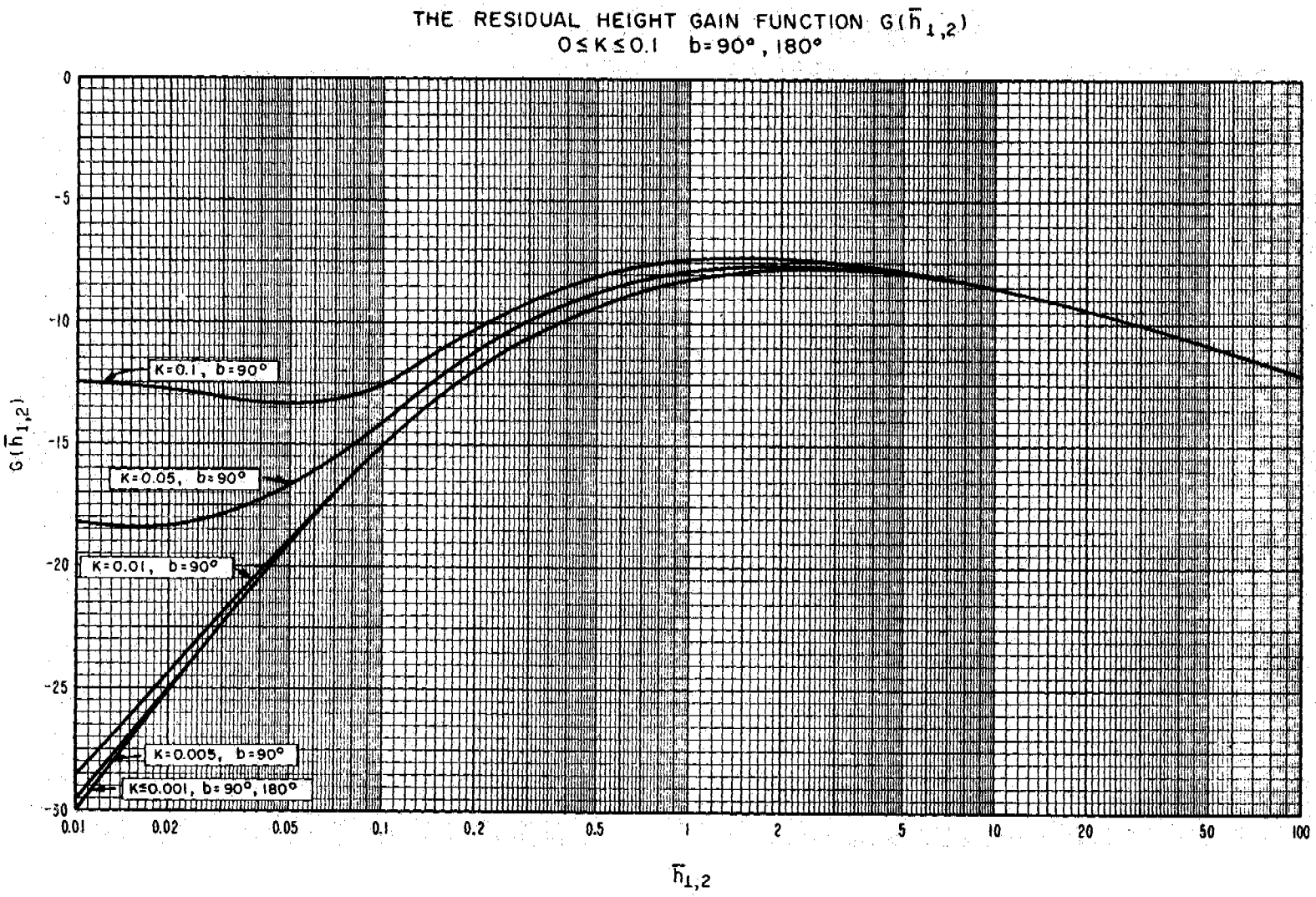
THE RESIDUAL HEIGHT GAIN FUNCTION $G(\bar{h}_{1,2})$
$0 \le K \le 0.1$ $b = 90°, 180°$
$G(\bar{h}_{1,2})$
0
-5
-10
-15
-20
-25
-30
K=0.1, b=90°
K=0.05, b=90°
K=0.01, b=90°
K=0.005, b=90°
K≤0.001, b=90°, 180°
0.01
0.02
0.05
0.1
0.2
0.5
1
2
5
10
20
50
100
$\bar{h}_{1,2}$

Figure 7.2

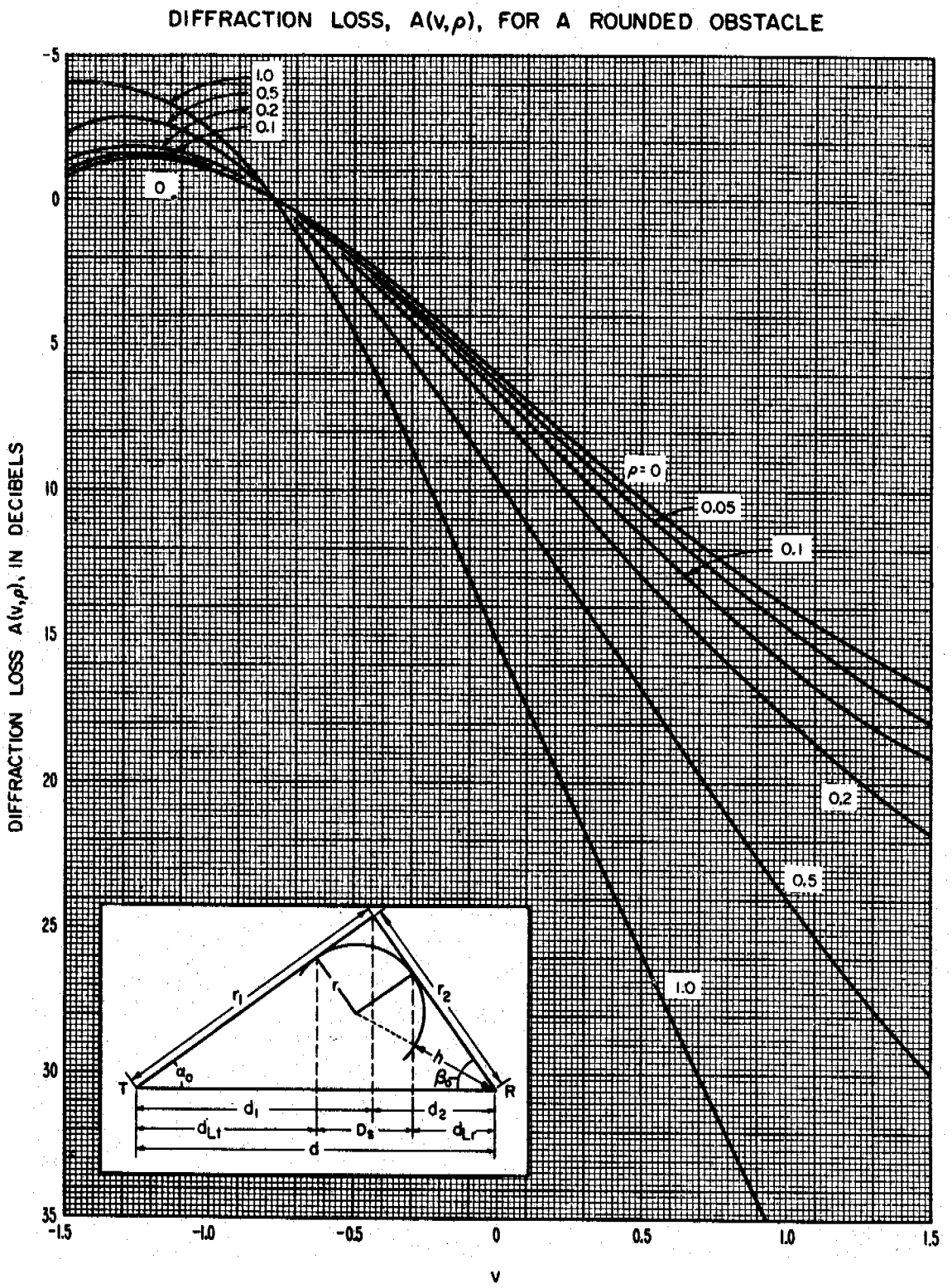
DIFFRACTION LOSS, A(v,ρ), FOR A ROUNDED OBSTACLE
DIFFRACTION LOSS A(v,ρ), IN DECIBELS
v
-5
0
5
10
15
20
25
30
35
-1.5
-1.0
-0.5
0
0.5
1.0
1.5
1.0
0.5
0.2
0.1
0
ρ = 0
0.05
0.1
0.2
0.5
1.0
T
R
r1
r
r2
h
α0
β0
d1
d2
dL1
Ds
dLr
d

Figure 7.3

INTERCEPT MAGNITUDE AND PHASE FOR DIFFRACTION
OVER A ROUNDED OBSTACLE

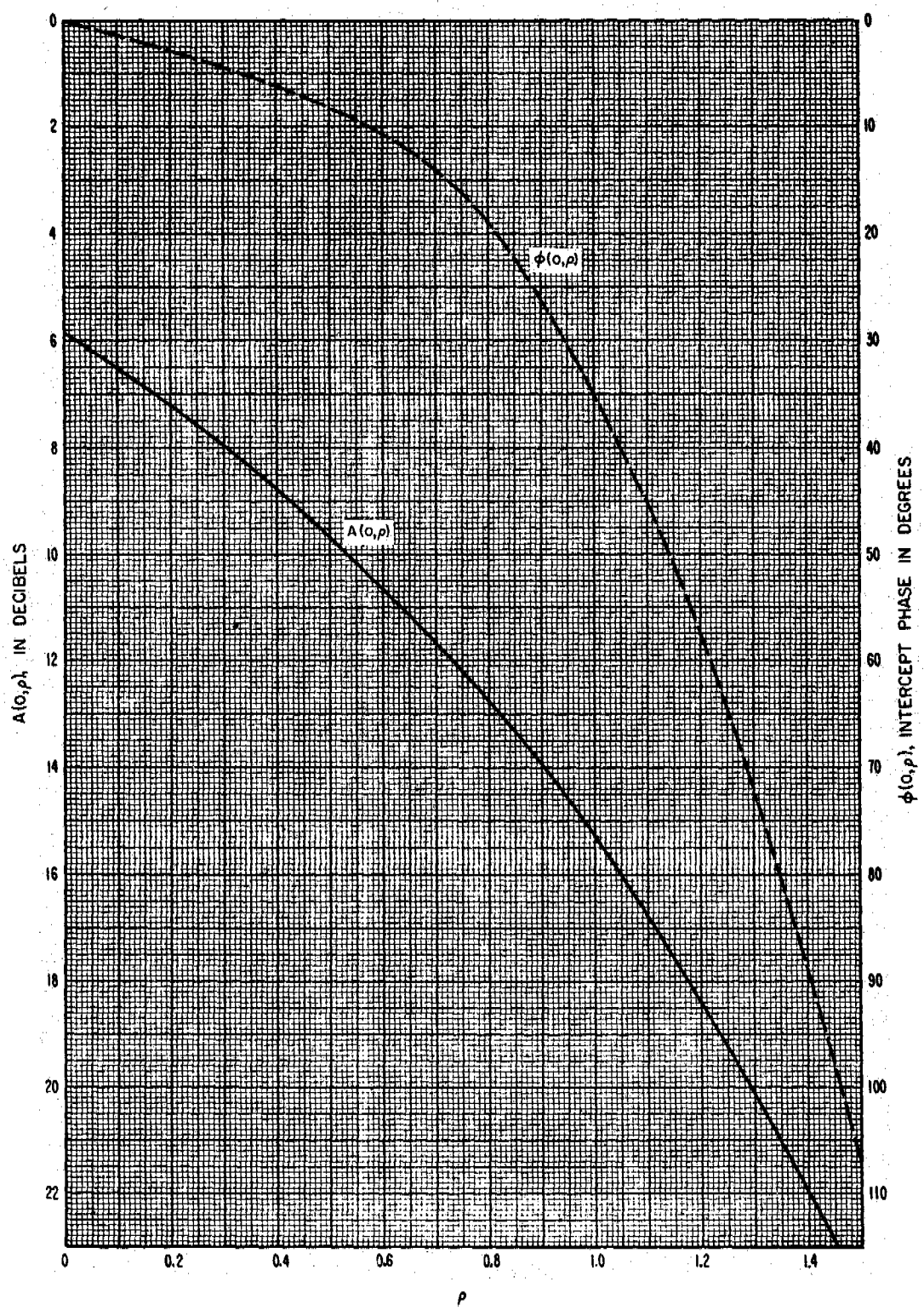

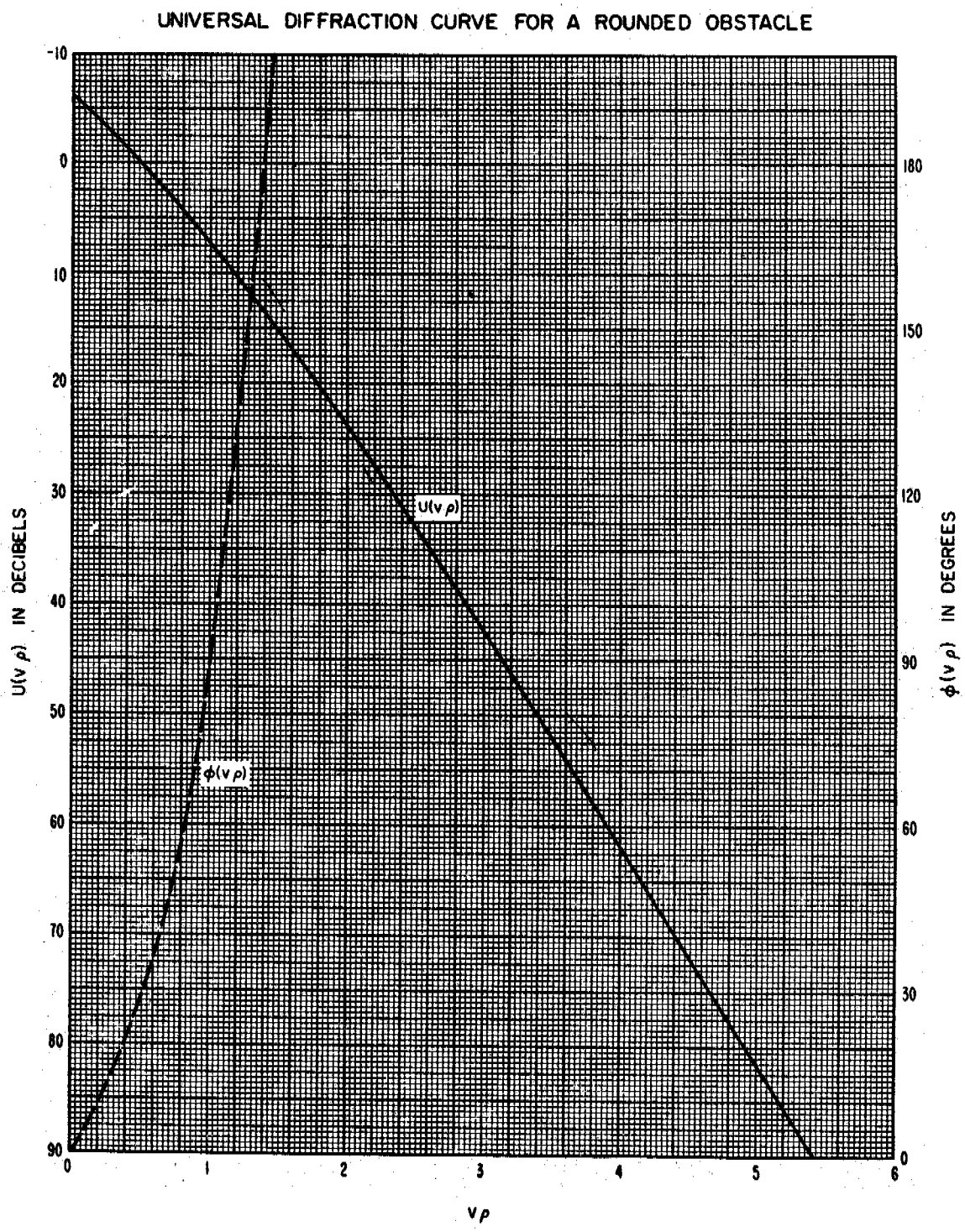
UNIVERSAL DIFFRACTION CURVE FOR A ROUNDED OBSTACLE
U(v ρ) IN DECIBELS
φ(v ρ) IN DEGREES
U(v ρ)
φ(v ρ)
-10
0
10
20
30
40
50
60
70
80
90
180
150
120
90
60
30
0
0
1
2
3
4
5
6
vρ

Figure 7.5

TERRAIN PROFILE FOR COLORADO KNIFE-EDGE DIFFRACTION PATH

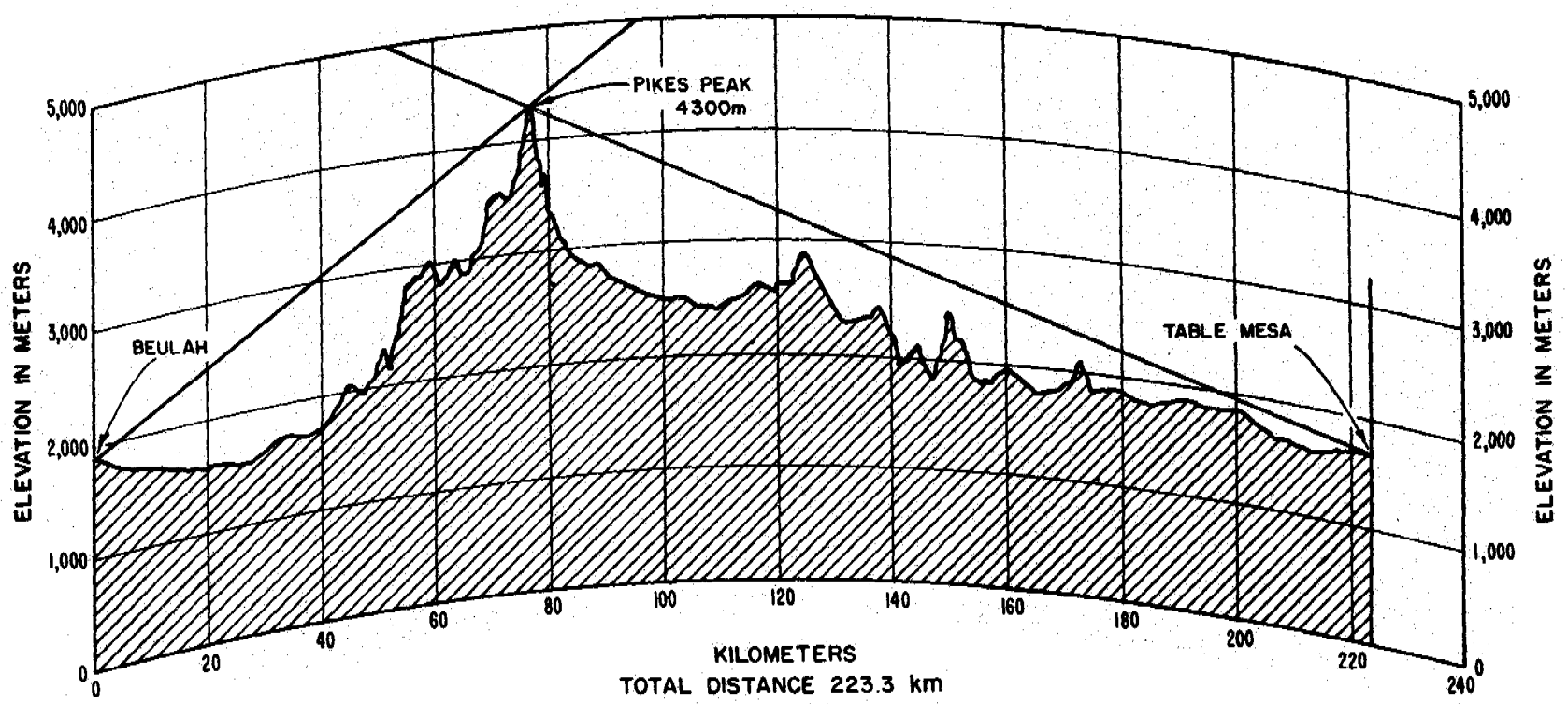


Figure 7.6

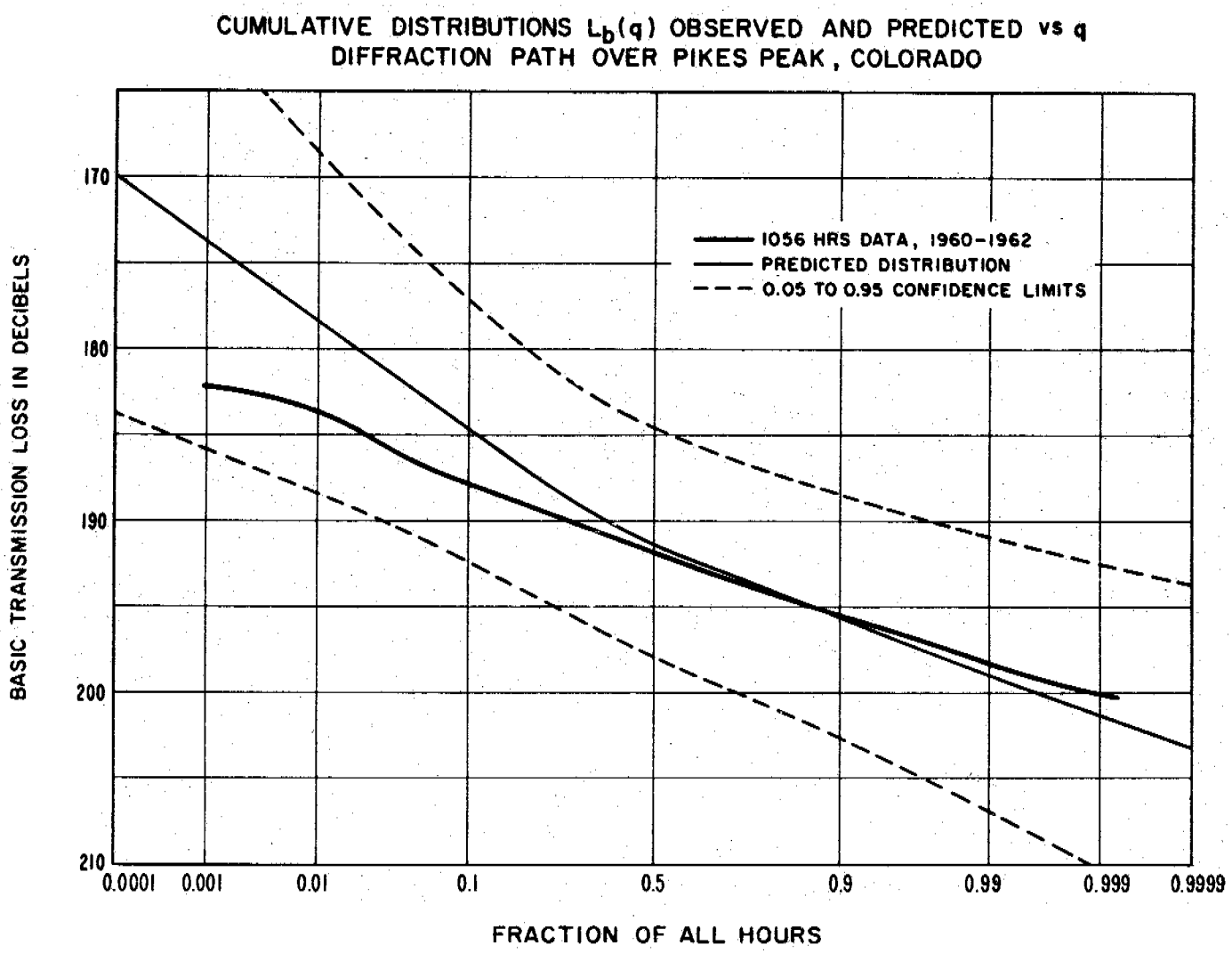
CUMULATIVE DISTRIBUTIONS $L_b(q)$ OBSERVED AND PREDICTED vs q
DIFFRACTION PATH OVER PIKES PEAK, COLORADO
1056 HRS DATA, 1960-1962
PREDICTED DISTRIBUTION
0.05 TO 0.95 CONFIDENCE LIMITS
BASIC TRANSMISSION LOSS IN DECIBELS
170
180
190
200
210
0.0001
0.001
0.01
0.1
0.5
0.9
0.99
0.999
0.9999
FRACTION OF ALL HOURS

Figure 7.7